Determination of the Load Spectrum of a Railway Track during the Operation of a Railroad Excavator

Vesna Jovanović*[1], Dragoslav Janošević[1], Dragan Marinković[2,3], Nikola Petrović[1], Jovan Pavlović[1]

[1]University of Niš, Faculty of Mechanical Engineering,
A. Medvedeva 14, 18000 Niš, Serbia; vesna.jovanovic@masfak.ni.ac.rs, dragoslav.janosevic@masfak.ni.ac.rs, nikola.petrovic@masfak.ni.ac.rs, jovan.pavlovic@masfak.ni.ac.rs

[2]Technical University Berlin, Institute of Mechanics, 17. Juni 135, 10623 Berlin, Germany; Dragan.Marinkovic@TU-Berlin.de

[3]Institute of Mechanical Science, Vilnius Gediminas Technical University, LT-10105 Vilnius, Lithuania; dragan.marinkovic@vilniustech-lt

* Corresponding author

Abstract: In this study, a mathematical model of a railroad excavator was developed, along with a program to determine the spectrum of allowable loads in the entire working space of the excavator, according to which determines the spectrum of possible track loads at the excavator's supports on the rails. The results show that the track loads vary and depend on the position of the excavator and the size of the load. The study's findings can inform the structural analysis of rail elements and the selection of manipulator tools to ensure excavator stability.

Keywords: railroad hydraulic excavators; load analysis, load spectrum

1 Introduction

Railway vehicles are vehicles that can move both on roads and on railway tracks. When operating on railway tracks, these vehicles retain their running gear, but are equipped with additional modules with steel wheels for track driving. The steel wheels are free and can be raised and lowered as needed. Rail vehicles are used for maintenance, repair or reconstruction of tracks, weed removal, cleaning and removal of waste from the tracks. They are also used in intermediate operations during track assembly and dismantling. The efficient use of heavy equipment on the railway is an important factor in the performance of works [1], and the choice of machines and mechanization plays a key role in the quality and productivity of railway maintenance. Today's industry offers modern machines for various types of railway work, which differ in functionality, degree of mechanization, productivity, accuracy. The efficiency of using these machines is a major factor for their use in track repair and maintenance. Efficiency criteria include cost reduction, increased capacity, speed of movement, reduced train hauling costs, extended time between repairs, and cost-effectiveness of track repairs. Meeting these criteria requires complex mechanization and proper selection [2, 3].

Railroad excavators (Fig. 1) are specialized machines designed for construction and maintenance tasks on railway tracks.

Figure 1
Railroad excavator: a) physical model b) possible manipulator tools

The advantage of using them lies in the various tools with which the same model of railroad excavator can be equipped to perform specific tasks [4]. On the other hand, the hydraulic systems of the excavators allow for precise and efficient handling, even in delicate tasks, which is crucial for the safe and efficient movement of trains. There are several types of movement mechanisms for railroad excavators [5]. The first type uses the existing wheels of conventional excavators and can only be used under conditions where the track gauge and the excavator's wheel spacing are the same. The other two types use attachments as special modules for moving the excavator on tracks, with one using the excavator's drive system and the other having an independent drive system. With the aim of increasing the cost-effectiveness and operational efficiency of these machines in railway construction and maintenance, Kwon et al. [5] discuss the development of a new traveling mechanism for railroad excavators based on a 14-ton class excavator. This new mechanism focuses on improving hydraulic performance and efficiency, validated through both experimental and simulation methods.

With the continuous increase in railway mileage, the demands and needs for efficient and safe maintenance of railway infrastructure [6-9] are also growing, which implies autonomous robot integration in railways infrastructure maintenance [10-13] or developing smart tools, i.e., robotizing existing human-operated on-track machines [14]. Therefore, the idea proposed by Di Natali et al. [14] is to develop control methods and toolboxes to transform any brand of hydraulic-rail excavator into an autonomous mobile on-track robot.

A significant portion of research attention is also directed towards the lateral stability of railway vehicle [15] and the interaction and dynamic force between the wheel and the rail [16]. Kazemian et al. [16] conducted a field test to investigate and compare the results of two different strain gauge arrangements and accelerometer installation positions, focusing on their differences in measuring the dynamic force between the wheel and the rail.

In the research by Shi et al. [17], experimental field tests were conducted to investigate how heavy loads induced by large axle loads influenced the dynamic behavior of the railway track. It is demonstrated that the various speed and axle load changes affect to the wheel-rail dynamic force, dynamic deformation of the track structure, and track vibration behavior. Furthermore, Han et al. [18] built a three-dimensional wheel–rail rolling contact model with a wheel flat to analyze the wheel–rail impact response induced by the wheel flat. Also, wheel wear is a serious concern for railroads due to the high cost of wheel reshaping, rail wear, and safety issues in operation [19, 20]. Great attention is also paid to the study of contact behavior between wheels and rails [21, 22]. Gupta et al. [21] focus on the numerical simulation of contact behavior between wheels and rails in a proposed road-cum-rail vehicle. Using the Finite Element Method and ANSYS software, the static behavior of the wheels is analyzed to predict parameters such as stress, deformation, and contact patch. The goal is to enhance the understanding of these interactions for the safe and efficient design of such vehicles. In this study, a mathematical model of a railroad excavator was developed, along with a program to determine the spectrum of allowable loads in the entire working space of the excavator, according to which determines the spectrum of possible track loads at the excavator's supports on the rails.

2 Mathematical Model

The mathematical model of a railroad excavatorfor analyzing the load spectrum on the track, when relying on its rails, is developed based on the physical model of the general configuration of the kinematic chain. This chain consists of the undercarriage - support moving member L_1 (Fig. 2), and the upper structure [23], which includes the rotary platform L_2, and the manipulator with booms L_3, L_4, the arm L_5, and the tool L_6. The support moving mechanism, through four metal wheels L_{11}, L_{12}, L_{13}, L_{14} enables the excavator to rely on and move along the railway track. The tool is attached to the end of the arm as a hook, grab, or gripper. The actuators of the boom and arm drive mechanism are bidirectional cylinders C_3 ,C_4 and C_5, directly connected to the pairs of kinematic pairs of the mechanism. The assumptions of the mathematical model are: a horizontal track base, the rails and members of the excavator's kinematic chain are rigid bodies; the members of the kinematic chain, kinematic pairs, and hydraulic cylinders of the drive mechanism are connected by fifth-class joints; the centers of mass of the kinematic chain members, hydraulic cylinders, and the load grasped by the tool, as well as the centers of the kinematic chain joints and drive mechanisms, lie in the longitudinal vertical plane of the kinematic chain in which the axis of the rotary platform lies; the centers of mass of the hydraulic cylinders are at the midpoint of the kinematic length of the hydraulic cylinders; the potential overturning lines of the railroad excavator are horizontal straight lines connecting the centers of support of the steel wheels and the track rails. The mathematical model of the railroad excavator is considered in an absolute coordinate system *OXYZ* with unit vectors *i*, *j*, *k* along the axes, where the horizontal plane *OXZ* lies in the contact plane of the moving mechanism and the track, with the *OX* axis normal to the track; the vertical *OY* axis coincides with the axis of rotation of the platform L_2, and the origin of the coordinate system coincides with the center of the support surface.

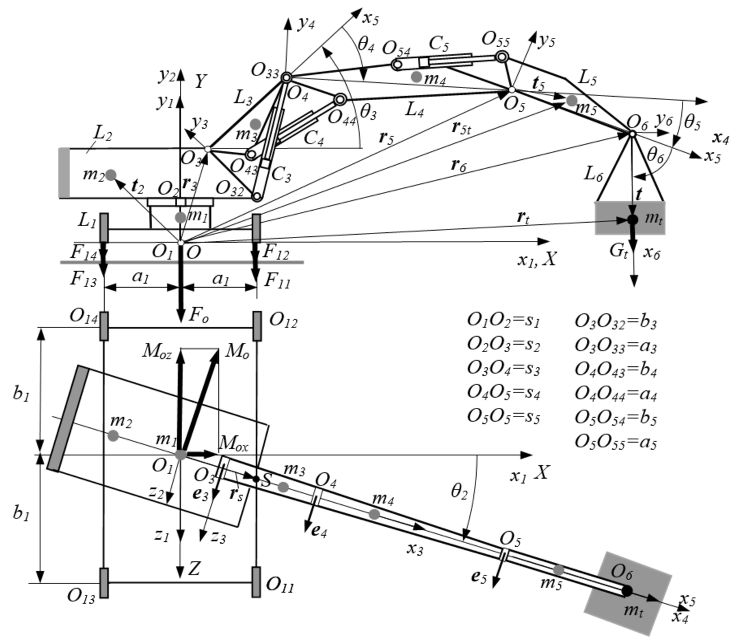

Figure 2
Mathematical model of railroad excavator

Each member of railroad excavator is defined in its local coordinate system $O_ix_iy_iz_i$, by a quantities [24]:

$$L_i = \{\hat{\boldsymbol{e}}_i, \hat{\boldsymbol{s}}_i, \hat{\boldsymbol{t}}_i, m_i\} \tag{1}$$

where are ***ei*** - the unit vectors of the axes of the rotational joints of the kinematic chain *Oi*, ***si*** - the position vector of joint O_{i+1} where member L_i connects to the next member (intensity vector is the length of the kinematic members) ***ti***- the position vector of the center of mass of member *Li*, *mi* – the mass of member.

Vectors in local coordinate systems are denoted with a hat above the symbol. The unit vectors of the axes of the rotational joints of the kinematic chain in the local coordinate systems of the chain members:

$$\hat{\boldsymbol{e}}_2 = \{0,1,0\},\ \hat{\boldsymbol{e}}_i = \{0,0,1\},\ \forall i = 3,4,5,6 \tag{2}$$

The drive mechanisms of the boom and arm are determined by a set of quantities:

$$C_i = \{d_{i1}, d_{i2}, \hat{\boldsymbol{a}}_i, \hat{\boldsymbol{b}}_i, c_{ip}, c_{ik}, p_{i1}, p_{i2}, m_{ci}, \eta_{cmi}, n_{ci}\}\ \forall i = 3,4,5 \tag{3}$$

where are d_{i1}, d_{i2} - the diameter of the piston/piston rod in the hydraulic cylinder, a_i, b_i - the vectors, i.e. coordinates, of the position of the centers of the joints in which the hydraulic cylinders are connected to the members of the drive mechanism kinematic pair, c_{ip}, c_{ik} - the initial and final length of the hydraulic cylinders, p_{i1},p_{i2} - the pressure in the supply and return lines of the hydraulic cylinder, η_{cmi} - the mechanical efficiency of the hydraulic cylinder, m_{ci}, n_{ci} - the mass and number of the hydraulic cylinder.

2.1 Geometric Quantities

The position of the excavator's kinematic chain is determined by a set of internal generalized coordinates:

$$\theta = \{\theta_1, \theta_2, \theta_3, \theta_4, \theta_5, \theta_6\} \tag{4}$$

where are $\theta_1 = 0^\circ$ - the angle of movement (lifting) of member L_1 relative to the horizontal *OXZ* plane, θ_2 - the angle of rotation of the local O_2x_2 axis of member L_2 relative to the O_1x_1 axis of member L_1 (angle for platform rotation), θ_3 , θ_4 - angles of rotation of the boom axes O_3x_3 and O_4x_3 relative to O_2x_2 platform axis, i.e. in relation to the axis O_3x_3, θ_5 - angles of rotation of the arm axes O_5x_5 axis of the arm relative to the O_4x_4 axis of the boom, θ_6 - the angle of position of the tool (with the load) axes O_5x_5 relative to the O_4x_4 axis of the arm.

The position of the excavator's kinematic chain is determined relative to the absolute coordinate system by a set of external generalized coordinates:

$$\varphi_1 = \theta_1 = 0,\ \varphi_2 = \theta_2,\ \varphi_3 = \theta_3,\ \varphi_4 = \theta_3 + \theta_4,\ \varphi_5 = \theta_3 + \theta_4 + \theta_5,\ \varphi_6 = -90^o \tag{5}$$

Vectors from the local coordinate systems $O_ix_iy_iz_i$ of the members of the kinematic chain are transformed into vectors in the absolute coordinate system *OXYZ* using a transformation matrix:

$$A_{01}=\begin{vmatrix}1 & 0 & 0\\ 0 & 1 & 0\\ 0 & 0 & 1\end{vmatrix}\ \forall L_1; \qquad A_{02}=\begin{vmatrix}cos\varphi_2 & 0 & -sin\varphi_2\\ 0 & 1 & 0\\ sin\varphi_2 & 0 & cos\varphi_2\end{vmatrix}\ \forall L_2; \tag{6}$$

$$A_{oi}=\begin{vmatrix}cos\varphi_i cos\varphi_2 & -sin\varphi_i cos\varphi_2 & -sin\varphi_2\\ sin\varphi_i & cos\varphi_i & 0\\ cos\varphi_i sin\varphi_2 & -sin\varphi_i sin\varphi_2 & cos\varphi_2\end{vmatrix}\ \forall L_3, L_4, L_5, L_6; \forall i=3,4,5,6 \tag{7}$$

The vectors $\boldsymbol{r}_i$ of the centers of the joints of the excavator's kinematic chain in the absolute coordinate system:

$$\boldsymbol{r}_i=\sum_2^i A_{oi-1}\widehat{\boldsymbol{s}}_{i-1}\ \ \forall i=2,...,6 \tag{8}$$

The vectors r_{ti} of the centers of mass of the members:

$$\boldsymbol{r}_{ti}=\boldsymbol{r}_i+A_{oi}\widehat{\boldsymbol{t}}_i\ \ \forall i=1,...,6 \tag{9}$$

and the vector of the center of the total mass of the tool and the load grasped by the excavator's tool in the absolute coordinate system:

$$\boldsymbol{r}_t=\boldsymbol{r}_6+A_{o6}\widehat{\boldsymbol{t}} \tag{10}$$

The vectors of the centers of the joints where the hydraulic cylinders are connected to the members of the kinematic pairs of the mechanism:

$$\boldsymbol{r}_{i,i-1}=\boldsymbol{r}_i+A_{oi-1}\widehat{\boldsymbol{b}}_i\ ,\boldsymbol{r}_{i,i}=\boldsymbol{r}_i+A_{oi}\widehat{\boldsymbol{a}}_i\ \ \forall i=3,4,5 \tag{11}$$

The vector r_s of the position of penetration point *S* of potential overturning lines through the longitudinal vertical plane of the excavator's kinematic chain rotated for the angle of the platform φ_2:

$$\boldsymbol{r}_s=\begin{Bmatrix} a_1\boldsymbol{i}+a_1 tg\varphi_2\boldsymbol{k}\ \ \forall\ 0\le\varphi_2\le arctg\dfrac{a_1}{b_1}\\ \dfrac{b_1}{tg\varphi_2}\boldsymbol{i}+b_1\boldsymbol{k}\ \ \ \forall\ \ arctg\dfrac{a_1}{b_1}\le\varphi_2\le\dfrac{\pi}{2}\end{Bmatrix} \tag{12}$$

The unit vector $\boldsymbol{e}_{ci}$ of the forces of the hydraulic cylinders of the boom and arm:

$$\boldsymbol{e}_{ci}=\frac{\boldsymbol{r}_{i,i}-\boldsymbol{r}_{i,i-1}}{\left|\boldsymbol{r}_{i,1}-\boldsymbol{r}_{i,i-1}\right|}\ \ \forall i=3,4,5 \tag{13}$$

2.2 Mechanical Quantities

By reducing all gravitational forces of the excavator's kinematic chain with the load weight G_t, the total allowable masses m_t attached to the tip of the excavator's manipulator, to the origin of the absolute coordinate system, in the plane of the excavator's support, the force vector $\boldsymbol{F_o}$ and the moment $\boldsymbol{M_o}$ are determined by the Eqs. (14) and (15):

$$\boldsymbol{F_o} = -g\left(m_t + \sum_{i=1}^{5} m_i + \sum_{i=3}^{5} m_{ci} \right)\boldsymbol{j} \tag{14}$$

$$\boldsymbol{M_o} = -g\left[\sum_{i=1}^{5} m_i(\boldsymbol{r}_{ti} \times \boldsymbol{j}) + \sum_{i=3}^{5} \frac{m_{ci}}{2}(\boldsymbol{r}_{i,i} \times \boldsymbol{j}) + \sum_{i=3}^{5} \frac{m_{ci}}{2}(\boldsymbol{r}_{i,i-1} \times \boldsymbol{j}) + m_t(\boldsymbol{r}_t \times \boldsymbol{j}) \right] \tag{15}$$

where are $m_t=m_6+m_{6t}$ - the total allowable mass of the load at the tip of the excavator's manipulator is equal to the sum of the mass of the tool m_6 and the mass of the load m_{6t} grasped by the tool.

The moment $\boldsymbol{M_s}$ of the gravitational forces of the excavator's kinematic chain, without the tool, for the penetration point S where the potential overturning line penetrates through the longitudinal vertical plane of the excavator at the angle φ_2 of platform rotation:

$$\boldsymbol{M_s} = -g\left[\sum_{i=1}^{5} m_i(\boldsymbol{r}_{ti} - \boldsymbol{r}_s) \times \boldsymbol{j} + \sum_{i=3}^{5} \frac{m_{ci}}{2}(\boldsymbol{r}_{i,i-1} - \boldsymbol{r}_s) \times \boldsymbol{j} + \sum_{i=3}^{5} \frac{m_{ci}}{2}(\boldsymbol{r}_{i,i} - \boldsymbol{r}_s) \times \boldsymbol{j} \right] \tag{16}$$

The moment $\boldsymbol{M_{oi}}$ of the gravitational forces of the excavator's kinematic chain, without the tool, for the center of joint O_3, O_4 and O_5:

$$\boldsymbol{M_{o3}} = -g\left[\sum_{i=3}^{5} m_i(\boldsymbol{r}_{ti} - \boldsymbol{r}_3) \times \boldsymbol{j} + \sum_{i=3}^{5} \frac{m_{ci}}{2}(\boldsymbol{r}_{i,i} - \boldsymbol{r}_3) \times \boldsymbol{j} + \sum_{i=4}^{5} \frac{m_{ci}}{2}(\boldsymbol{r}_{i,i-1} - \boldsymbol{r}_3) \times \boldsymbol{j} \right] \tag{17}$$

$$\boldsymbol{M_{o4}} = -g\left[\sum_{i=4}^{5} m_i(\boldsymbol{r}_{ti} - \boldsymbol{r}_4) \times \boldsymbol{j} + \sum_{i=4}^{5} \frac{m_{ci}}{2}(\boldsymbol{r}_{i,i} - \boldsymbol{r}_4) \times \boldsymbol{j} + \frac{m_{c5}}{2}(\boldsymbol{r}_{54} - \boldsymbol{r}_4) \times \boldsymbol{j} \right] \tag{18}$$

$$\boldsymbol{M_{o5}} = -g\left[m_5(\boldsymbol{r}_{t5} - \boldsymbol{r}_5) \times \boldsymbol{j} + \frac{m_{c5}}{2}(\boldsymbol{r}_{55} - \boldsymbol{r}_5) \times \boldsymbol{j} \right] \tag{19}$$

From the conditions of the static stability of the excavator, relative to the potential overturning lines, expressed by the equation Eq. (20):

$$\boldsymbol{M}_s \cdot \boldsymbol{e} + g \cdot k_s m_{ts}((\boldsymbol{r}_t - \boldsymbol{r}_s) \times -\boldsymbol{j}) \cdot \boldsymbol{e} = 0 \tag{20}$$

the total allowable load mass m_{ts} permitted by the stability of the excavator is determined:

$$m_{ts} = \frac{-\boldsymbol{M}_s \cdot \boldsymbol{e}}{g \cdot k_s \left(\left(\boldsymbol{r}_t - \boldsymbol{r}_s \right) \times -\boldsymbol{j} \right) \cdot \boldsymbol{e}} \tag{21}$$

where are $\boldsymbol{e}=\boldsymbol{e}_3=\boldsymbol{e}_4$ - the unit vectors normal to the longitudinal vertical plane of the excavator's kinematic chain, k_s - the coefficient of static stability of the excavator [25].

From the equilibrium conditions for the axes $O_i z_i$ ($i=3,4,5$) of the rotational joints of the drive mechanisms of the manipulator, expressed by the equation Eq. (22):

$$\boldsymbol{M}_{oi} \cdot \boldsymbol{e}_i + F_{ci} \left(\boldsymbol{e}_{ci} \times \boldsymbol{a}_i \right) \cdot \boldsymbol{e}_i + g \cdot k_h m_{ti} \left(\left(\boldsymbol{r}_t - \boldsymbol{r}_i \right) \times -\boldsymbol{j} \right) \cdot \boldsymbol{e}_i = 0 \quad \forall \; i = 3,4,5 \tag{22}$$

the total maximum load mass m_{ti} that each drive mechanism of the excavator manipulator can carry is determined:

$$m_{ti} = \frac{-\boldsymbol{M}_{oi} \cdot \boldsymbol{e}_i - F_{ci} \left(\boldsymbol{e}_{ci} \times \boldsymbol{a}_i \right) \cdot \boldsymbol{e}_i}{g \cdot k_h \left[\left(\boldsymbol{r}_t - \boldsymbol{r}_i \right) \times -\boldsymbol{j} \right] \cdot \boldsymbol{e}_i} \quad \forall \; i = 3,4,5 \tag{23}$$

where are k_h - the hydraulic safety factor of the excavator [25], F_{ci} - is the intensity of the force vector in the hydraulic cylinders C_3 ,C_4, and C_5 of the drive mechanism, determined by the equation Eq. (24):

$$F_{ci} = \begin{cases} \frac{\pi}{4} \left[d_{i1}^2 \cdot p_{i1} - \left(d_{i1}^2 - d_{i2}^2 \right) p_{i2} \right] \eta_{cmi} \cdot n_{ci} & \forall \; \boldsymbol{M}_{o3} \cdot \boldsymbol{e}_3 < 0, \boldsymbol{M}_{o4} \cdot \boldsymbol{e}_4 < 0, \boldsymbol{M}_{o5} \cdot \boldsymbol{e}_5 > 0, i = 3,4,5 \\ -\frac{\pi}{4} \left[\left(d_{i1}^2 - d_{i2}^2 \right) p_{i1} - d_{31}^2 \cdot p_{i2} \right] \eta_{cmi} \cdot n_{ci} & \forall \; \boldsymbol{M}_{o3} \cdot \boldsymbol{e}_3 > 0, \boldsymbol{M}_{o4} \cdot \boldsymbol{e}_4 > 0, \boldsymbol{M}_{o5} \cdot \boldsymbol{e}_5 < 0, i = 3,4,5 \end{cases} \tag{24}$$

The total allowable load mass m_t at the tip of the excavator manipulator, in a given position of the kinematic chain, has the value:

$$m_t = min \left\{ m_{ts}, m_{t3}, m_{t4}, m_{t5} \right\} \tag{25}$$

For the total allowable load mass m_t, at the supports O_{11}, O_{12}, O_{13}, O_{14} (Fig. 2) of the support movement mechanism of the excavator, the railway tracks are loaded with forces:

$$F_{11} = \frac{\boldsymbol{F}_o \cdot \boldsymbol{j}}{4} - \frac{\boldsymbol{M}_o \cdot \boldsymbol{i}}{4 b_1} + \frac{\boldsymbol{M}_o \cdot \boldsymbol{k}}{4 a_1} \tag{26}$$

$$F_{12} = \frac{\boldsymbol{F}_o \cdot \boldsymbol{j}}{4} + \frac{\boldsymbol{M}_o \cdot \boldsymbol{i}}{4 b_1} + \frac{\boldsymbol{M}_o \cdot \boldsymbol{k}}{4 a_1} \tag{27}$$

$$F_{13} = \frac{\boldsymbol{F}_o \cdot \boldsymbol{j}}{4} - \frac{\boldsymbol{M}_o \cdot \boldsymbol{i}}{4 b_1} - \frac{\boldsymbol{M}_o \cdot \boldsymbol{k}}{4 a_1} \tag{28}$$

$$F_{14} = \frac{\boldsymbol{F_o} \cdot \boldsymbol{j}}{4} + \frac{\boldsymbol{M_o} \cdot \boldsymbol{i}}{4b_1} - \frac{\boldsymbol{M_o} \cdot \boldsymbol{k}}{4a_1} \tag{29}$$

3 Analysis

Based on the previously defined mathematical model, a program has been developed to determine the load spectrum of the railway track during the operation of a hydraulic railroad excavator supported on the railway tracks.

The program is given a set of parameters for the members of the kinematic chain L_i and the drive mechanism C_i of the railway excavator, as well as the desired number of positions of the railroad excavator in the entire working space. By changing the rotation angle of the platform and the strokes of the hydraulic cylinders of the drive mechanism, the program first determines the geometric quantities: the coordinates of the joint centres and the mass centres of the members of the excavator's kinematic chain.

Then, in each position of the railway excavator, the following are calculated: the total maximum load mass m_{4s} from the stability conditions of the excavator and the total maximum load masses m_{ti} ($i=3,4,5$) from the hydraulic stability conditions of the drive mechanisms of the manipulator. Finally, based on the allowable total load mass m_t, the forces F_{1i} ($i=1,...,4$) in the supports of the excavator that load the track are determined.

As an example, using the developed program, the load spectrum of the railway track was determined for a hydraulic railroad excavator with a mass of approximately *22,000* kg, with the parameters of the kinematic chain and drive mechanisms (Table 1) corresponding to the models of the world's leading excavator manufacturers (Liebherr, Caterpillar, Komatsu, Atlas) that are most used.

The program simulated the computational model of the excavator during the transfer of the load suspended at the tip of the arm L_5 in the working space within the interval of the platform rotation angle φ_2=[$0°,90°$].

Table 1

Parameters of the calculation model of the excavator (Fig. 2)

Parameter name	Label	Size	Dimension
Coordinates of the kinematic length s_1 of the member L_1	s_{1x}/s_{1y}	0/1150	mm
Track width	$2 \times a_1$	2×717	mm
Railway wheel span	$2 \times b_1$	2×2400	mm
Member mass L_1	m_1	9000	kg

Coordinates of the kinematic length s_2 of the member L_2	s_{2x}/ s_{2y}	570/860	mm
Member mass L_2	m_2	7800	kg
Kinematic length s_3 of the member L_3	s_3	1630	mm
Member mass L_3	m_3	1000	kg
Kinematic length s_4 of the member L_4	s_4	3210	mm
Member mass L_4	m_4	1500	kg
Kinematic length s_5 of the member L_5	s_5	2200	mm
Member mass L_5	m_5	625	kg
Diameter of hydraulic cylinder piston/rod c_3	$2xd_{31}/d_{32}$	2×100/70	mm
Diameter of hydraulic cylinder piston/rod c_4	d_{41}/d_{42}	180/90	mm
Diameter of hydraulic cylinder piston/rod c_5	d_{51}/d_{52}	140/80	mm
Mechanical efficiency of hydraulic cylinders	η_{cm}	0.96	-
Pressure in the supply/return lines of hydraulic cylinders	p_{31}/ p_{32}	33/1	MPa

During the spatial simulation, by changing the platform rotation angle (with a step of $\varphi_2=2°$), the position of the longitudinal vertical plane of the manipulator changes.

In the separated working space of the excavator and the entire working field, 5,000 positions of the members of the excavator's kinematic chain were observed in the plane of the manipulator. The obtained results for the entire working space of the excavator are presented in the form of spectra of the allowable load capacity of the excavator and the load on the railway track, depending on the platform rotation angle and the coordinates of the excavator's working field.

The spectrum (Fig. 3a) of the total allowable load at the tip of the excavator manipulator shows that the allowable load weight G_t changes with the change in the platform rotation angle φ_2. Additionally, for each platform rotation angle in the entire working field, the allowable load weight varies within the range of minimum and maximum values. The change in the allowable load weight occurs due to the change in the position of the excavator's kinematic chain relative to the potential overturning lines and the change in the relative position of the kinematic chain members due to movement while performing functions in the working field.

It is characteristic that the maximum values of the allowable load weight are lower in the zone of transverse positions of the excavator's kinematic chain compared to the zone of longitudinal positions of the kinematic chain, observed in relation to the potential overturning lines, respectively, direction of the railway track on which the excavator is supported.

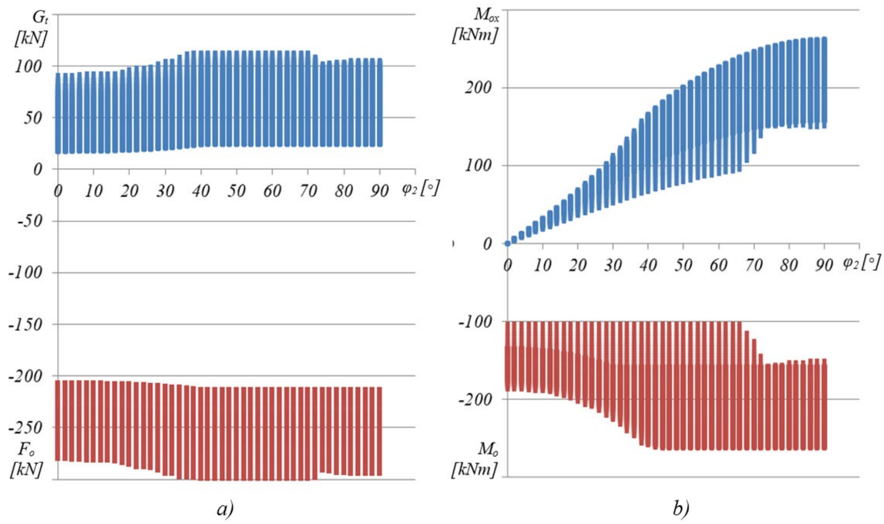

Figure 3

The spectra of changes in the working space of the excavator: a) allowable load weight G_t and total reduced force F_o at the center of the excavator's support surface, b) reduced moment M_o and the component M_{ox} of the reduced moment depending on the platform position angle φ_2

Higher values of the maximum allowable load weight in the zone of longitudinal positions of the excavator's kinematic chain are possible due to the greater stability moment of the excavator, as the centres of mass of the support moving member and the platform are further from the overturning line, given that the distance ($2b_1$) between the transverse overturning lines is greater than the distance ($2a_1$) between the longitudinal overturning lines ($2b_1 > 2a_1$, Fig. 2).

The spectrum of changes (Fig. 3b) in the minimum and maximum values of the reduced force F_o at the centre of the support surface, depending on the platform rotation angle φ_2, is similar to the change in the allowable load weight, which, together with the gravitational forces of the kinematic chain, determines its intensity. Given the nature of the changes in the allowable load weight, the reduced force F_o has higher values in the zone of longitudinal positions of the kinematic chain compared to the transverse positions in the working space of the excavator.

The spectrum of the reduced moment M_o (Fig. 3b) depending on the platform rotation angle φ_2 shows that the maximum moment values are in the zone of longitudinal positions of the excavator's kinematic chain. For the observed working space of the excavator ($\varphi=0^o$- 90^o), with the increase in the angle φ_2, the component M_{ox} (Fig. 3a) of the moment M_o increases, while the component M_{oz} has an inverse change pattern.

The spectra of the reduced force F_o (Fig. 4) depending on the coordinates (X_6, Y_6) of the reach of the manipulator top in the working field, when the excavator is in the transverse position at a platform angle $\varphi_2=0°$ (Fig. 4a) and in the longitudinal position at an angle $\varphi_2=90°$ (Fig. 4b), show that the highest values of the force F_o are possible when the manipulator is in the area of minimal horizontal reach and the lowest when the area of maximum horizontal and vertical reach in the working field of the excavator.

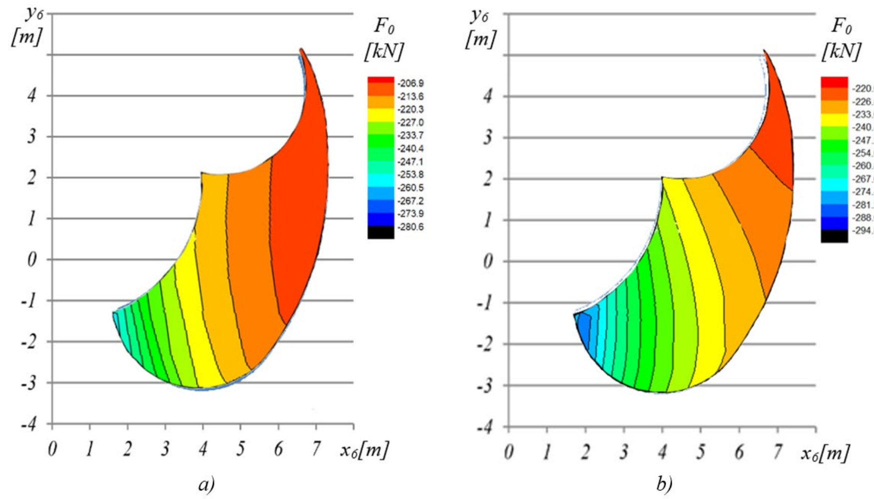

Figure 4

The spectra of the reduced force F_o depending on the coordinates of the manipulator's reach in the working field of the excavator for the platform position angle: a) $\varphi_2=0°$, b) $\varphi_2=90°$

The spectra of the reduced moment M_o (Fig. 5) depending on the coordinates (X_6, Y_6) of the reach of the manipulator top in the working field, when the excavator is in the transverse position at a platform angle $\varphi_2=0°$ (Fig. 5a) and in the longitudinal position at an angle $\varphi_2=90°$ (Fig. 5b), show that the highest values of the moment M_o can occur when the manipulator is in the area of minimal horizontal reach below the support plane of the excavator and the lowest in the area of maximum horizontal and vertical reach in the working field above the support plane of the excavator. By comparing the spectra, it is observed that in the longitudinal position of the excavator at a platform angle $\varphi_2=90°$, the highest reduced moments M_o can occur for the manipulator's reach in a significantly larger area of the working field compared to the transverse position of the excavator at an angle $\varphi_2=0°$.

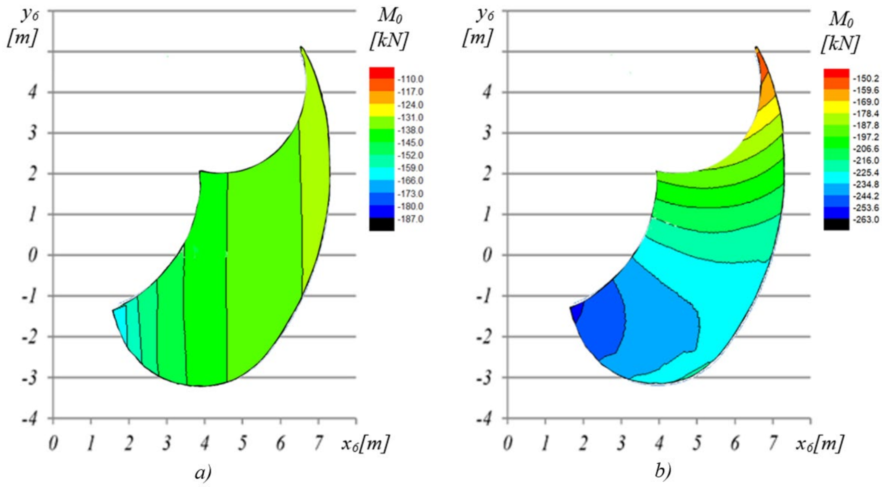

Figure 5

The spectra of the reduced moment M_o depending on the coordinates of the manipulator's reach in the working field of the excavator for the platform position angle: a) $\varphi_2=0°$, b) $\varphi_2=90°$

The obtained spectra of the forces F_{11}, F_{12}, F_{13}, F_{14} (Fig. 6) with which the excavator loads the track at the supports O_{11}, O_{12}, O_{13}, O_{14} show that in the observed working space, depending on the platform rotation angle φ_2, they have distinctly different characteristics and intensity of changes. In addition to the reduced force F_o, the reduced moment M_o significantly affects the difference in the intensity of the force changes. Since the polygon formed by the potential overturning lines of the excavator is rectangular, the action of the reduced force F_o is equally divided into components that load the track at the supports of the excavator. The forces by which the reduced moment M_o acts on the track depend on the direction of its components M_{ox}, M_{oz}, and the distance $2a_1$ between the longitudinal and the distance $2b_1$ between the transverse potential overturning lines of the excavator, observed in relation to the direction of the track. In the observed working area of the excavator, within the interval of platform rotation angle changes ($\varphi_2=0°$-$90°$), the spectra of forces F_{11} and F_{14} that load the rail at supports O_{11} and O_{14} are characteristic. In the zone of transverse positions of the excavator's kinematic chain, the track is loaded only by forces F_{11}, F_{12}, while at supports O_{13}, O_{14} there is no track load $F_{13}=F_{14}=0$. This type of rail load case occurs because in the zone of the transverse positions of the excavator, the components M_{oz} of the moment M_o are greater than the components of M_{ox}. Since in this zone $2a_1<2b_1$, the forces from the action of the M_{oz} moment, which load the rail, are greater in intensity than the force in the supports O_{13}, O_{14} resulting from the action of the force F_o and the components M_{ox} of the opposite direction, which leads to the unloading of the rail in the supports O_{13}, O_{14} ($F_{13}=F_{14}=0$) and increased loading of the rail in the supports O_{11}, O_{12}. According to the given force spectra, the maximum possible rail load is at support O_{11} (Fig. 6a) when the longitudinal vertical plane of the kinematic chain, i.e., the excavator platform, is rotated by an angle of $\varphi_2=38^o$.

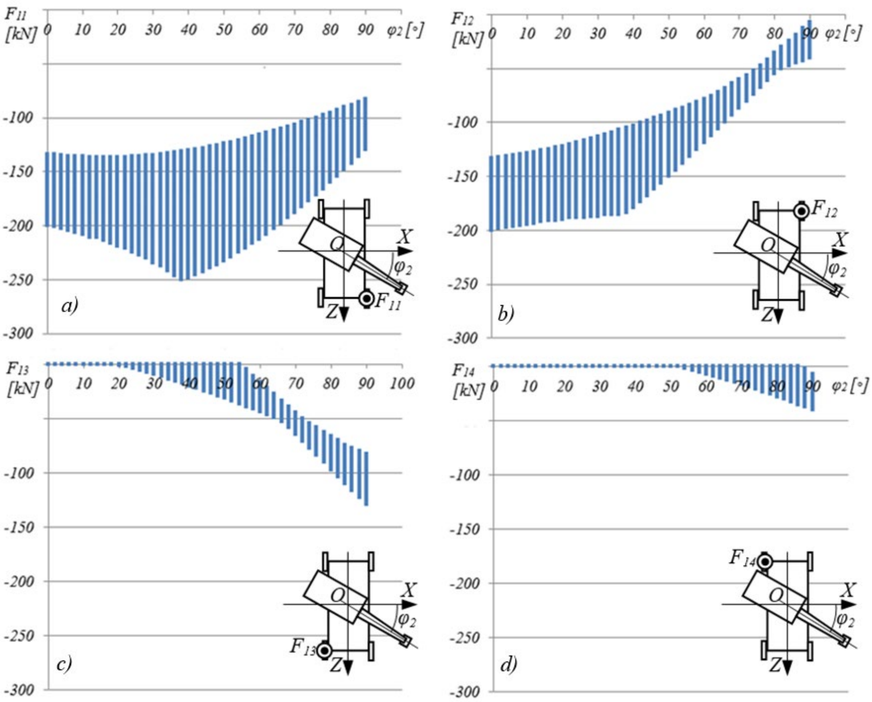

Figure 6

Spectra of force changes in the working area of the excavator that load the rail: a) F_{11},b) F_{12},c) F_{13}, d) F_{14} depending on the angle of the platform position φ_2

The spectrum of the intensity of the force F_{11} (Fig. 7a) depending on the coordinates (X_6, Y_6) of the reach of the manipulator top in the working field when the excavator is in the position at the platform angle $\varphi_2=38^o$, shows that the highest values of the force F_{11} occur when the horizontal reaches of the manipulator in the working field (area A) are minimal below the level of the excavator support. From the spectrum of the allowable total mass m_t of the load (Fig. 7b), given depending on the coordinates (X_6, Y_6) of the reach of the manipulator top in the working field when the excavator is in the position at the platform angle $\varphi_2=38^o$, it is observed that the maximum values of the force F_{11}, which load the rail, occur at the highest values of the allowable total mass m_t of the load in area A of the working field when the manipulator's horizontal reaches are minimal.

The same spectrum shows that the minimum values of the allowable mass m_t of the load occur at the maximum horizontal and vertical reaches of the manipulator in the working field of the excavator, when possible and smaller values of the force F_{11} that load the rail in the support O_{11}.

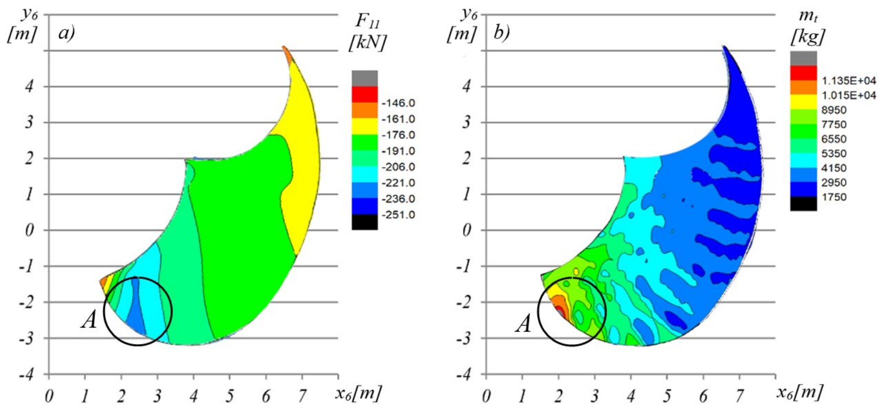

Figure 7

Spectra: a) of force F_{11}, b) allowable total load mass mt depending on the coordinates of the reach of the manipulator in the working field of the excavator for the angle of the platform position $\varphi_2=38°$

Conclusion

Hydraulic excavators with a support movement mechanism for moving and supporting railway tracks are used to perform numerous functions in the development and maintenance of railway infrastructure.

This study analyzed the load on the railway track when the excavator, supported on the rails, performs load transfer functions with tools of various shapes (grab, hook, clamp). A mathematical model of the railroad excavator was defined, and a program was developed to determine the spectrum of allowable loads in the entire manipulative space of the excavator, according to which, the spectrum of possible rail loads at the excavator supports on the rails is formed. The results obtained in the study show that the load on the railway track at the supports of the excavator on the rails is variable and depends on the position and size of the load handled by the manipulator tool, the shape and dimensions of the polygon formed in the support plane by the potential overturning lines of the excavator, and the position of the kinematic chain of the excavator relative to the potential overturning lines of the railroad excavator. In general, in addition to the analysis of rail loads, the loading spectra can be used as initial data for the structural analysis of rail elements and their substrate. Furthermore, according to the load spectra of the hydraulic excavator supported on the railway tracks, the sizes of various manipulator tools that do not compromise the stability of the excavator in the entire working space can be reliably selected.

Acknowledgement

This research was financially supported by the Ministry of Education, Science and Technological Development of the Republic of Serbia (Contract No. 451-03-9/2021-14/200109).

References

[1] Kurniawan, M. A., Dewi, P., Adi, W. T., Subagio, A.: Optimization of heavy equipment usage for railway track works, ICORT, 220, 2023 pp. 146-155, https://doi.org/10.2991/978-94-6463-126-5_16

[2] Ilinykh, A. S., Kolyasov, K. M., Yaitskov, I. A.: Assessing the effectiveness of track operation mechanization facilities, Transportation Research Procedia, 61, 2022, pp. 668-673, https://doi.org/10.1016/j.trpro.2022.01.106

[3] Sasidharan, M., Burrow, M. P., N., Ghataora, G. S.: A whole life cycle approach under uncertainty for economically justifiable ballasted railway track maintenance, Research in Transportation Economics, 80, 2020, https://doi.org/10.1016/j.retrec.2020.100815

[4] Jovanović, V., Janošević, D., Marinković, D., Petrović, N., Pavlović, J.: Railway load analysis during the operation of an excavator resting on the railway track, Acta Polytechnica Hungarica 20(1), 2023, pp. 79-93

[5] Kwon, J., Lee, M.: Development of traveling equipment for construction and maintenance of railroad track based on 14-ton class excavator, International Journal of Engineering Technologies and Management Research, 5(2), 2018, pp. 1-9, https://doi.org/10.29121/ijetmr.v5.i2.2018.141

[6] Fischer, S., Harangozó, D., Németh, D., Kocsis, B., Sysyn, M., Kurhan, D., Brautigam, A.: Investigation of heat-affected zones of thermite rail weldings, Facta Universitatis series: Mechanical Engineering, 22(4), 2024, pp. 689-710, https://doi.org/10.22190/FUME221217008F

[7] Li, J., Durazo-Cardenas, I., Ruiz-Carcel, C., He, F., Anderson, R., Hall, A., Burbridge, D., Starr, A.: Smart railways: the design and construction of an autonomous inspection and maintenance vehicle, Procedia CIRP, Volume 128, 2024, pp. 61-65, ISSN 2212-8271, https://doi.org/10.1016/j.procir.2024.03.003

[8] Fischer, S.: Investigation of the Settlement Behavior of Ballasted Railway Tracks Due to Dynamic Loading, Spectrum of mechanical engineering and operational research, 2(1), 2025, pp. 24-46, https://doi.org/10.31181/smeor21202528

[9] Ézsiás, L., Tompa, R., Fischer, S.: Investigation of the Possible Correlations between Specific Characteristics of Crushed Stone

Aggregates, Spectrum of Mechanical Engineering and Operational Research, 1(1), 2024, pp.10-26, https://doi.org/10.31181/smeor1120242

[10] Rahman, M., Liu, H., Masri, M., Durazo-Cardenas, I., Starr, A.: A railway track reconstruction method using robotic vision on a mobile manipulator: A proposed strategy, Computers in Industry, 148, 2023, 0166-3615, https://doi.org/10.1016/j.compind.2023.103900

[11] Brautigam, A., Szalai, S., Fischer S.: Investigation of the application of austenitic filler metals in paved tracks for the repair of the running surface defects of rails considering field tests, Facta Universitatis series: Mechanical Engineering, online first, https://casopisi.junis.ni.ac.rs/index.php/FUMechEng/article/view/12081

[12] Liu, H., Rahman, M., Rahimi, M., Starr, A., Durazo-Cardenas, I., Ruiz-Carcel, C., Ompusunggu, A., Hall, A., Anderson, R.: An autonomous rail-road amphibious robotic system for railway maintenance using sensor fusion and mobile manipulator, Computers and Electrical Engineering, 110, 2023, https://doi.org/10.1016/j.compeleceng.2023.108874

[13] Eller, B., Fischer, S.: Application of concrete canvas for enhancing railway substructure performance under static and dynamic loads, Facta Universitatis series: Mechanical Engineering, online first, https://casopisi.junis.ni.ac.rs/index.php/FUMechEng/article/view/12081

[14] Di Natali, C., Mattila, J., Kolu, A., De Vito, P., Gauttier, S., Morata, M., Garcia, M., Caldwell, D.: Smart tools for railway inspection and maintenance work, performance and safety improvement, Transportation Research Procedia, 72, 2023, pp. 3070-3077, https://doi.org/10.1016/j.trpro.2023.11.856

[15] Bhardawaj, S., Sharma, C. R., Sharma, K. S.: Development in the modeling of rail vehicle system for the analysis of lateral stability, Materials Today: Proceedings, Volume 25, Part 4, 2020, pp. 610-619, ISSN 2214-7853, https://doi.org/10.1016/j.matpr.2019.07.376

[16] Kazemian, M., Rad, M. M., Shadfar, M., Doost, M. A., Raisi, H. E., Fischer, S.: Optimum train weighing in motion using inertial sensors, Acta Polytechnica Hungarica 21(1), 2024, pp. 221-240

[17] Shi, Z., Wang, K., Zhang, D., Chen, Z., Zhai, G., Huang, D.: Experimental investigation on dynamic behaviour of heavy-haul railway track induced by heavy axle load, Transport, 34(3), 2019, pp. 351-362, https://doi.org/10.3846/transport.2019.10325

[18] Han, L., Jing, L., Liu, K.: A dynamic simulation of the wheel–rail impact caused by a wheel flat using a 3-D rolling contact model, J. Mod. Transport. 25, 2017, pp. 124-131, https://doi.org/10.1007/s40534-017-0131-0

[19] Corrêa, H. A. P., Ramos, G. P., Fernandes, R., Kurka, R. G. P., Antunes dos Santos, A.: Effect of primary suspension and friction wedge maintenance parameters on safety and wear of heavy-haul rail vehicles, Wear, 2023, pp. 524-525, https://doi.org/10.1016/j.wear.2023.204748

[20] Tian, S., Luo, X., Ren, L., & Xiao, C.: Active steering control strategy for rail vehicle based on minimum wear number. Vehicle System Dynamics, 59(8), 2020, pp. 1256-1281, https://doi.org/10.1080/00423114.2020.1743864

[21] Gupta, A., Pradhan, K. S., Bajpai, L., Jain, V.: Numerical simulation of contact behavior between rail wheel and rails of a new road cum rail vehicle, Materials Today: Proceedings, 46(9), 2021, pp. 3966-3974, https://doi.org/10.1016/j.matpr.2021.02.523

[22] Sharma, S. K., Kumar, A.: Dynamics Analysis of Wheel Rail Contact Using FEA, Procedia Engineering, Volume 144, 2016, pp. 1119-1128, ISSN 1877-7058, https://doi.org/10.1016/j.proeng.2016.05.076

[23] Jovanović, V., Janošević, D., Marinković, D., Petrović, N.: Djokić, R.: Analysis of influential parameters in the dynamic loading and stability of the swing drive in hydraulic excavators, Machines 2024, 12, 737, https://doi.org/10.3390/machines12100737

[24] Jovanović, V., Janošević, D., Marinković, D., Petrović, N.: Influential factors in the loading of the axial bearing of the slewing platform drive in hydraulic excavators, Technical Gazette 30(1), 2023, pp. 158-168, https://doi.org/10.17559/TV-20220425205603

[25] ISO 10567:2007, Earth-moving machinery - Hydraulic excavators - Lift capacity